J. Fluid Mech. (1991), vol. 224, pp. 159–175
Printed in Great Britain

Inviscid spatial stability of a compressible mixing layer. Part 3. Effect of thermodynamics

By T. L. JACKSON[1] AND C. E. GROSCH[2]

[1] Department of Mathematics and Statistics, Old Dominion University, Norfolk, VA 23529, USA

[2] Department of Oceanography and Department of Computer Science, Old Dominion University, Norfolk, VA 23529, USA

(Received 26 June 1989 and in revised form 12 July 1990)

We report the results of a comprehensive comparative study of the inviscid spatial stability of a parallel compressible mixing layer using various models for the mean flow. The models are (i) the hyperbolic tangent profile for the mean speed and the Crocco relation for the mean temperature, with the Chapman viscosity–temperature relation and a Prandtl number of one; (ii) the Lock profile for the mean speed and the Crocco relation for the mean temperature, with the Chapman viscosity–temperature relation and a Prandtl number of one; and (iii) the similarity solution for the coupled velocity and temperature equations using the Sutherland viscosity–temperature relation and arbitrary but constant Prandtl number. The purpose of this study was to determine the sensitivity of the stability characteristics of the compressible mixing layer to the assumed thermodynamic properties of the fluid. It is shown that the qualitative features of the stability characteristics are quite similar for all models but that there are quantitative differences resulting from the difference in the thermodynamic models. In particular, we show that the stability characteristics are sensitive to the value of the Prandtl number and to a particular value of the temperature ratio across the mixing layer.

1. Introduction

The study of the stability of compressible shear flows is somewhat more complicated than that of incompressible shear flows in that the thermodynamics of the compressible fluid is of major importance. As a consequence of compressibility the types of disturbances which can exist are quite varied: they can be subsonic, sonic, or supersonic modes and these can be either vorticity or acoustic modes (Mack 1984, 1987, 1989); there can be multiple unstable modes with the same frequency; and finally three-dimensional modes are of great importance because they may be more unstable than two-dimensional modes; the characteristics of these modes are dependent upon the thermodynamics chosen.

The earliest calculations of stability characteristics of compressible boundary layers used realistic thermodynamic relations (Brown 1962; Lees & Reshotko 1962; Mack 1965) and this has continued to be the practice to the present day. The situation with regard to stability calculations for free shear layers is quite different. Most studies of the stability of compressible free shear flows have been based on assumed, somewhat arbitrary, mean velocity and temperature profiles which are not solutions to the mean flow equations but do satisfy the boundary conditions. If both the velocity and temperature profiles are arbitrary it might be conjectured that the

solutions of the stability problem could be unrelated to those of the physical problem. If they are, at least, rough approximations to the actual solutions, one might conjecture that the solutions of the model stability problem would approximate those of the physical problem. These solutions of the model problems might be useful in elucidating qualitative features of the true stability problem because they are easier to treat. Some examples of studies of this type are that of Gill (1965), who studied the temporal stability of 'top hat' jets and wakes; those of Blumen (1970), Blumen, Drazin & Billings (1975), and Drazin & Davey (1977) who examined the temporal stability of a compressible mixing layer with the mean velocity profile assumed to be given by a hyperbolic tangent and a constant temperature profile; and Djordjevic & Redekopp (1988) who studied temporal stability with a hyperbolic tangent velocity profile and varying temperature.

In most compressible free shear stability studies the thermodynamics used was that of the model fluid (Stewartson 1964). This model was originally introduced in order to simplify the thermodynamics of the flow in compressible boundary layers. In addition to obeying the perfect gas law (valid for real gases at temperatures less than a few thousand degrees K), the model fluid has a unit Prandtl number so that the rates of diffusion of heat and momentum are equal, and the Chapman (1950) viscosity law with the viscosity proportional to the temperature is assumed to be valid. One class of approximate solutions involves modelling the mean velocity profile by a hyperbolic tangent and using the Crocco relation for the mean temperature profile. This approximation has been used by a number of authors, including Ragab & Wu (1988), Tam & Hu (1988, 1989), and Zhuang, Kubota & Dimotakis (1988). We have also used this model in a comprehensive study of the spatial stability of an unbounded compressible mixing layer (Jackson & Grosch 1989; hereinafter referred to as Part 1), a bounded compressible mixing layer (Jackson & Grosch 1990*a*) as well as in a similar study of a reacting compressible mixing layer (Jackson & Grosch 1990*b*).

Another class of models can be defined as those which use the Lock profile (Lock 1951), the similarity solution for the velocity profile with the viscosity proportional to the temperature, a Prandtl number of one and various temperature profiles. Lessen, Fox & Zien (1965, 1966) in temporal stability calculations used the Lock profile and assumed that the flow was iso-energetic so that the temperature of the stationary gas was much greater than that of the moving gas even at moderately supersonic speeds. Gropengiesser (1969) used a generalized hyperbolic tangent profile (see his equation (2.27)) to approximate the Lock profile and used the Crocco relation for the temperature in spatial stability calculations.

The final class of solutions to the mean flow equations are those where the Prandtl number is not necessarily one and a reasonably realistic viscosity–temperature relation, such as the Sutherland law, is used. The velocity and temperature profiles are exact similarity solutions of the mean flow equations. Quite surprisingly, there are few linear stability calculations for compressible mixing layers with these more realistic mean velocity and temperature profiles. The only published results, of which we know, are those of Ragab & Wu (1988) for spatial stability and those of Macaraeg, Streett & Hussaini (1988) for temporal stability. It seems that the main interest of Ragab & Wu was to determine the dependence of the maximum growth rate of the disturbances on the velocity ratio of the mixing layer for subsonic flows. They concluded that the maximum growth rate depends on the velocity ratio in a complex way. Macaraeg *et al.* studied the temporal stability of a compressible mixing layer for a few selected values of the Mach number ($\leqslant 4$), and a few values of the free-stream

temperature ratio. They were the first to point out the sensitivity of the stability characteristics of this class of flows to variations in the Prandtl number.

Very recently there has been a revival of interest in the stability of compressible free shear layers, particularly at supersonic speeds. An unanswered question is the accuracy of the results of those calculations in which various models of the mean flow thermodynamics have been used. It is clear that there will be quantitative differences in, for example, phase speeds and growth rates of the disturbances depending on the model of the mean flow. The important questions are first, the extent to which qualitative predictions of recent, and older, studies are dependent on the models of the mean velocity and temperature used, and second, the magnitude of the differences in the quantitative predictions as a function of the mean flow model.

In order to answer these questions we undertook a comprehensive systematic study of the stability of one free shear flow, the compressible mixing layer. In this study we calculated the stability characteristics of the compressible mixing layer using a number of representative models of the mean velocity and temperature profiles over a wide range of Mach numbers. The models are (i) the hyperbolic tangent profile for the mean speed and the Crocco relation for the mean temperature, with the Chapman viscosity–temperature relation and a Prandtl number of one; (ii) the Lock profile for the mean speed and the Crocco relation for the mean temperature, with the Chapman viscosity–temperature relation and a Prandtl number of one; and (iii) the similarity solution for the coupled velocity and temperature equations using the Sutherland viscosity temperature relation and arbitrary but constant Prandtl number. In §2 we formulate the problem, including defining the thermodynamic models. Our results are presented in §3. Finally, we summarize our conclusions in §4.

2. Formulation of the problem

2.1. *The mean flow*

The problem considered here is the inviscid spatial stability of the steady two-dimensional flow of a compressible mixing layer which lies between two streams with different speeds and temperatures. We take one of the streams to be moving at $+\infty$ and the other to be stationary at $-\infty$. The equations are non-dimensionalized by the values of the density, temperature, and speed in the moving stream. The lengthscale is a characteristic length of the mean flow, and the timescale is the ratio of the length and speed scales. The x-axis is along the direction of flow, the y-axis is normal to the flow direction, and the z-axis is in the cross-stream direction. U and V are the velocity components in the x and y directions, respectively, ρ is the density, and T the temperature. We assume that the equations governing the mean flow are the compressible boundary-layer equations (Stewartson 1964). The equations for the mean flow quantities $U = f'(\eta)$ and T are given by

$$\left(\frac{\mu}{T}f''\right)' + 2ff'' = 0, \tag{2.1}$$

$$\left(\frac{\mu}{Pr\,T}T'\right)' + 2fT' + (\gamma-1)M^2\left(\frac{\mu}{T}\right)(f'')^2 = 0, \tag{2.2}$$

where the primes indicates differentiation with respect to the similarity variable η, and the Howarth–Dorodnitzyn transformation has been used. Here μ is the viscosity

coefficient, Pr is the Prandtl number, γ is the ratio of specific heats of the gas, and M the Mach number of the moving stream. The appropriate boundary conditions are

$$f'(+\infty) = 1, \quad T(+\infty) = 1, \quad f'(-\infty) = 0, \quad T(-\infty) = \beta_T, \tag{2.3}$$

with β_T the ratio of the temperature in the stationary gas to that of the moving gas. If β_T is less than one, the stationary stream is relatively cold compared to the moving stream, and if β_T is greater than one it is relatively hot.

It should be noted that (2.1)–(2.3) constitute a fifth-order boundary-value problem, but that there are only four boundary conditions. Ting (1959) has shown that an appropriate boundary condition can be obtained by matching the free-stream pressures on either side of the mixing layer if at least one of the steams is supersonic. However, Klemp & Acrivos (1972) have shown that this condition is incomplete if both streams are subsonic. These conditions are equivalent to a specification of $f(-\infty)$. This value, a specification of the stream function, can be varied so as to ensure that $f(0)$ takes on any particular value. This will not effect the physics of the flow, only the location of the origin of the coordinate system.

The structure of the mean flow clearly depends on the variation of μ and Pr with temperature and pressure. In general, both μ and Pr are very weakly dependent on pressure and can be taken to be independent of pressure. The Prandtl number is somewhat dependent on the temperature but, for this study, will be assumed to be constant, with calculations being carried out over a range of Pr between 0.7 and 1.0. Finally, the dependence of viscosity on temperature is quite important and the choice of that dependence leads to several thermodynamic models discussed in the following section.

2.2. *Flow models*

Given a value of Pr and $\mu(T)$ the mean flow is determined by the solution to (2.1) and (2.2) with the boundary conditions (2.3) and a specification of $f(0)$. We will consider three models for the mean flow.

If it is assumed that the viscosity is proportional to the temperature, that is we use the Chapman viscosity law, (2.1) is uncoupled from (2.2). With $Pr = 1$, (2.2) can be solved in closed form to give the Crocco relation, which with the boundary conditions (2.3), is given by

$$T = 1 - (1 - \beta_T)(1 - U) + \tfrac{1}{2}(\gamma - 1) M^2 U(1 - U). \tag{2.4}$$

The first model of the mean flow involves using (2.4) for the mean temperature profile and approximating the mean velocity profile by a hyperbolic tangent

$$U = \tfrac{1}{2}(1 + \tanh(\eta)). \tag{2.5}$$

We will call this approximation the Tanh model. The results for this model were presented in Part 1. Some of these results will be reproduced here for ease of reference and comparison purposes. The second model of the mean flow again uses (2.4) for the mean temperature profile, and the solution to (2.1) with μ proportional to T and $Pr = 1$, for the mean velocity profile. We will call this the Lock model. The third model is one in which the Prandtl number is constant but not necessarily one and a reasonably realistic viscosity–temperature relation is used. For temperatures greater than about 100 K, a Sutherland type of relation

$$\mu = aT^{\frac{3}{2}}/(b + T), \quad a = 1 + b, \quad b = 110.4\ \mathrm{K}^\circ/T^*, \tag{2.6}$$

with T^* the reference temperature, is reasonably accurate. The mean velocity and

temperature profiles are the solutions of (2.1)–(2.3) and μ given by (2.6). We will call this the Sutherland model. Typical velocity and temperature profiles are shown in figure 1 for $\beta_T = \frac{1}{2}$, Mach 2, and two values of the Prandtl number. The shapes of these profiles are quite similar, but as will be shown below these small differences can have substantial effects on the stability properties.

2.3. *The stability problem*

The stability problem can be formulated independently of the detailed form of the U and T profiles. The flow field is perturbed by introducing two-dimensional wave disturbances in the velocity, pressure, temperature and density with amplitudes which are functions of η. It is straightforward to derive a single equation governing the amplitude of the pressure perturbation Π, given by

$$\Pi'' - \frac{2U'}{U-c}\Pi' - \alpha^2 T[T - M^2(U-c)^2]\Pi = 0, \tag{2.7}$$

where c is the complex phase speed

$$c = \frac{\omega}{\alpha}, \tag{2.8}$$

and primes indicate differentiation with respect to the similarity variable η. The stability problem is thus to solve (2.7) for a given real frequency ω and Mach number M. The eigenvalue is the complex wavenumber α. The real part of α is the wavenumber in the x-direction, while the imaginary part of α indicates whether the disturbance is amplified, neutral, or damped depending on whether α_i is negative, zero, or positive. If α_i is zero, $c = c_N$ is the phase speed of a neutral mode.

The boundary conditions for Π are obtained by considering the limiting form of (2.7) as $\eta \to \pm\infty$. The solutions to (2.7) are of the form

$$\Pi \to \exp(\pm\Omega_\pm \eta), \tag{2.9}$$

where

$$\Omega_+^2 = \alpha^2[1 - M^2(1-c)^2], \quad \Omega_-^2 = \alpha^2\beta_T[\beta_T - M^2c^2]. \tag{2.10}$$

We define $c_\pm$ to be the values of the phase speed for which $\Omega_\pm^2$ vanishes. Thus,

$$c_+ = 1 - \frac{1}{M}, \quad c_- = \frac{(\beta_T)^{\frac{1}{2}}}{M}. \tag{2.11}$$

Note that c_+ is the phase speed of a sonic disturbance in the moving stream and c_- is the phase speed of a sonic disturbance in the stationary stream. At

$$M = M_* \equiv 1 + (\beta_T)^{\frac{1}{2}}, \tag{2.12}$$

$c_\pm$ are equal, and this value is denoted $\hat{c}$.

A more detailed discussion of the stability problem can be found in Part 1. We only note here that the classification scheme in regards to figure 1 of Part 1 will also be used here to classify the instabilities.

Since (2.7) has a singularity at $U = c_N$, we integrate it along the complex contour $(-\eta_-, -1)$ to $(0, -1)$ and $(\eta_+, -1)$ to $(0, -1)$ using a variable step Runge–Kutta scheme. In our calculations we have taken $\eta_\pm$ to be 6 for the Tanh and Lock models. However, we found that η_- needs to be larger for the Sutherland model because the

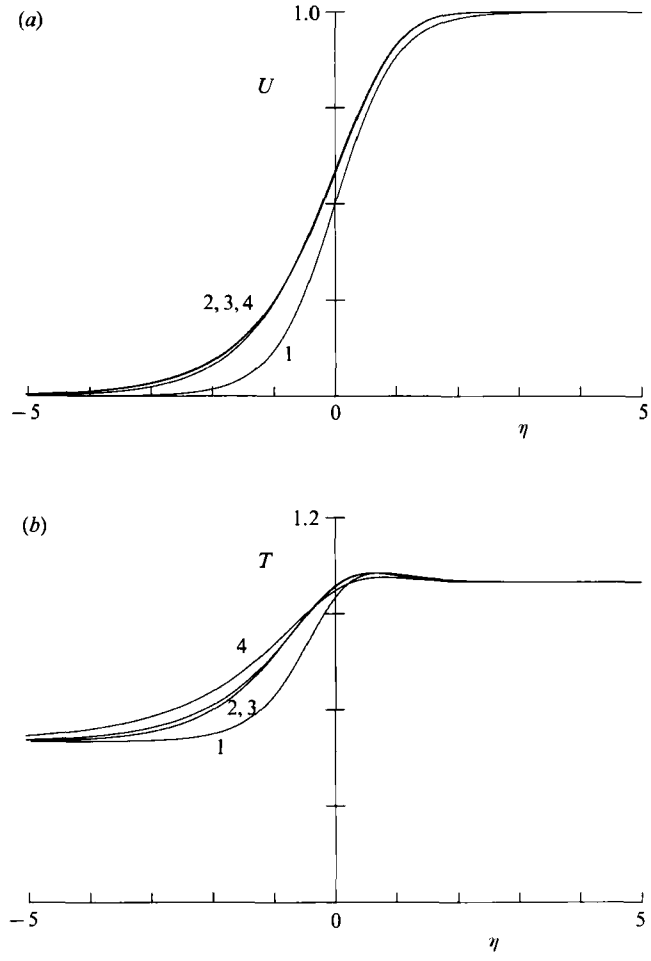

FIGURE 1. Plot of the (*a*) velocity and (*b*) temperature *vs.* η for $\beta_T = \frac{1}{2}$, Mach 2, and thermodynamic models (1) Tanh, (2) Lock, (3) Sutherland with $Pr = 1.0$, and (4) Sutherland with $Pr = 0.7$.

decay at $-\infty$ is slower than for the other two models, with the rate of decay decreasing as β_T is decreased (Mack 1989). We choose an initial value of α and compute the boundary conditions as in Part 1. We then iterate on the wavenumber α, using Muller's method, until the boundary conditions are satisfied and the jump in the solution at $(0, -1)$ is less than 10^{-6}. All calculations were done in 64 bit precision. Various numerical tests showed that the eigenvalues are correct to at least one part in 10^5.

3. Results

In this section we present results for the regularity condition, phase speeds, and growth rates of the stability problem. In all of our calculations we have taken $\gamma = 1.4$ and $0 \leqslant M \leqslant 7$. We have also taken the reference temperature T^* to be 1500 K. Stability calculations for values of T^* of 500 K and 1000 K were done and it was found that there was at most only a 2% change in the eigenvalues. Thus, we conclude that the actual value of the reference temperature T^* is not the important

parameter, rather it is the ratio, β_T, of the temperatures in the stationary stream to that of the moving stream which is the important parameter.

3.1. *The regularity condition*

The Lees & Lin (1946) regularity function is defined by

$$S(\eta) \equiv \frac{\mathrm{d}}{\mathrm{d}\eta}\left(T^{-2}\frac{\mathrm{d}U}{\mathrm{d}\eta}\right). \tag{3.1}$$

Let η_c be a root of $S(\eta)$, and define $\tilde{c} = U(\eta_c)$. If $\tilde{c}$ lies in region 1 of the $c_r - M$ diagram (see figure 1, Part 1), then Lees & Lin (1946) have shown that, provided $\alpha \neq 0$, $\tilde{c} = c_N$ is the phase speed of a true neutral mode. This condition is a generalization of the Rayleigh condition for incompressible shear flow (Drazin & Reid 1984). The corresponding neutral wavenumber and frequency must be determined numerically. These modes are called subsonic neutral modes. If $\tilde{c}$ lies in regions 2, 3 or 4 of the $c_r - M$ diagram, then $\tilde{c}$ does not correspond to the phase speed of a true neutral mode. The phase speeds in these regions must be found numerically.

We have shown analytically in Part 1, for the Tanh model, that S is a cubic in tanh (η) and therefore has either one or three real roots. These roots depend on the Mach number, β_T, and γ. There is one real root for $M < M_0$ and three real roots for $M \geqslant M_0$, where M_0 is a function of β_T and γ, and is given by (3.6) of Part 1. For $\beta_T = 1$, there is a single real root with phase speed of $\frac{1}{2}$ (denoted by $\hat{c}$) and is independent of Mach number. If $\beta_T > 1$ the value of $\hat{c}$ for the single root is a monotonically increasing function of the Mach number, with a value always greater than $\hat{c}$. On the other hand, if $\beta_T < 1$, the value of $\hat{c}$ for the single root is a monotonically decreasing function of the Mach number, with a value always less than $\hat{c}$. Thus $\beta_T = 1$ is a transition value. This unique value of β_T, which we denote by $\hat{\beta}_T$, plays a critical role in the behaviour of the solutions of the stability problem, as will be shown below. The corresponding value of the root which appears at Mach zero has been denoted by $\hat{c}$.

We have not been able to demonstrate the above properties analytically for the Lock and Sutherland models, but have been able to do so numerically. For the Lock model the transition value is $\hat{\beta}_T = 0.57753$, with $\hat{c} = 0.4318$. For the Sutherland model with $Pr = 1$ the transition value is $\hat{\beta}_T \approx 0.445$ with $\hat{c} \approx 0.392$, while for $Pr = 0.7$ the transition value is $\hat{\beta}_T \approx 0.164$ with $\hat{c} \approx 0.252$. Since the mean profiles of velocity and temperature are coupled through the viscosity for the Sutherland model, the exact transition value was difficult to determine numerically. It is clear that the value of $\hat{\beta}_T$ is strongly dependent on the value of the Prandtl number. The dependence on Pr is shown very clearly in the results presented in figure 2 where we plot $\hat{\beta}_T$ and $\hat{c}$ for the Sutherland model as a function of the Prandtl number. Note that as the Prandtl number is decreased from one, the transition values of $\hat{\beta}_T$ and $\hat{c}$ also decrease.

For all three thermodynamic models the three real roots of S always lie in regions 2, 3, or 4 for two-dimensional modes. Therefore, for a two-dimensional mode, only the single root which lies in region 1 is the phase speed of a true neutral mode. However, the sonic speeds $c_\pm$ are functions of the angle of propagation of the waves (see (2.20), Part 1), and as the angle is increased, the sonic curves shift towards higher Mach numbers thus increasing the extent of region 1. It is therefore clear that there will be some angle of propagation for which all three zeros of S lie in region 1. For this angle and all greater angles less than 90°, all three zeros of S yield the phase speed of true neutral subsonic modes.

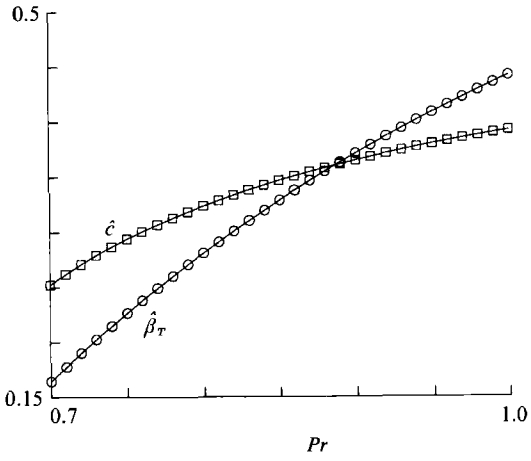

FIGURE 2. Plot of ○, $\hat{\beta}_T$ and □, $\hat{c}$ *vs.* Prandtl number for the Sutherland model.

3.2. *Neutral modes*

In this section we present the phase speeds, frequencies, and wavenumbers of the neutral modes for the three models with β_T of 2.0, 1.0, and 0.5 and $Pr = 0.7$ for the Sutherland model.

We have shown in the previous section that if $\hat{c}$ lies in region 1, then it corresponds to the phase speed of a true subsonic neutral mode, denoted by c_N. For any of the three thermodynamic models, if $\beta_T = \hat{\beta}_T$, the phase speed of the neutral mode is independent of Mach number in region 1. This is true for Mach numbers up to M_*, where the mode splits into a pair of supersonic neutral modes, one in region 2 and the other in region 4. If $\beta_T > \hat{\beta}_T$, the phase speed of the subsonic neutral mode increases with Mach number up to M_s, the Mach number at which the phase speed equals that of the sonic wave. Beyond M_s the subsonic neutral mode of region 1 is transformed into a fast supersonic neutral mode in region 2. In addition, at M_* a slow supersonic neutral mode appears in region 4. If $\beta_T < \hat{\beta}_T$, then the opposite behaviour occurs.

Figure 3 shows plots of the phase speeds of the neutral modes as a function of Mach number for $\beta_T = 2$ obtained by using the Tanh, Lock, and Sutherland models. The results for all three models show qualitatively similar behaviour and small quantitative differences. It should be noted that β_T of 2.0 is considerably larger than the transition value of $\hat{\beta}_T$ for all three models. There are some quantitative differences between the results using the different models. For example, in region 1, the neutral mode of the Tanh model has the lowest phase speed and that of the Lock model the highest with the phase speed of the Sutherland model in between. However, there is only about a 10% maximum difference in the phase speeds. The same ordering with respect to magnitude of the phase speed is also true for the fast supersonic neutral mode in region 2. The phase speeds of the slow supersonic neutral modes in region 4 are very nearly the same for all of the models over the range of Mach numbers shown. The wavenumbers and frequencies of the neutral modes show very similar behaviour with Mach number for all the models.

Similar results are shown in figure 4 for $\beta_T = 1.0$. One can see a marked difference between the results for the Tanh model and the others. This is due to the fact that $\hat{\beta}_T = 1$ is the transition value for the Tanh model. Thus the phase speed of the subsonic neutral mode of the Tanh model is constant up to $M_s = M_*$ where the mode

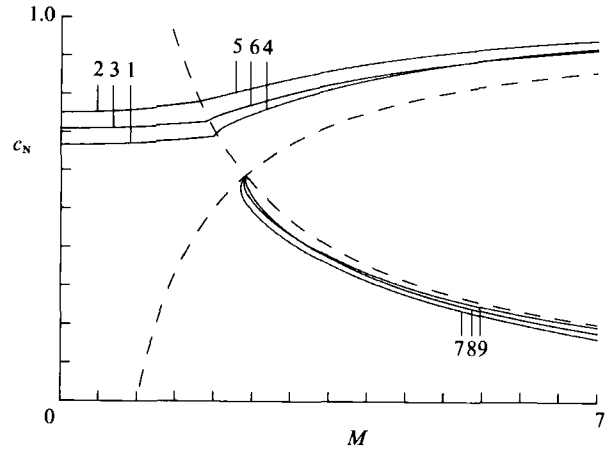

FIGURE 3. Plots of two-dimensional neutral phase speeds for $\beta_T = 2.0$ *vs.* Mach number: ——, phase and – – –, sonic speeds; subsonic modes: (1) Tanh, (2) Lock, (3) Sutherland; fast modes: (4) Tanh, (5) Lock, (6) Sutherland; slow modes: (7) Tanh, (8) Lock, (9) Sutherland.

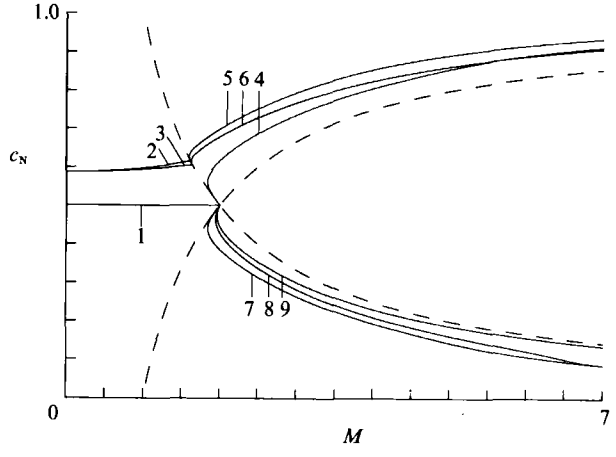

FIGURE 4. Plots of two-dimensional neutral phase speeds for $\beta_T = 1.0$ *vs.* Mach number: ——, phase and – – –, sonic speeds; subsonic modes: (1) Tanh, (2) Lock, (3) Sutherland; fast modes: (4) Tanh, (5) Lock, (6) Sutherland; slow modes: (7) Tanh, (8) Lock, (9) Sutherland.

then splits into fast and slow supersonic neutral modes. The phase speeds of the subsonic neutral modes for the Lock and Sutherland models increase slightly as M increases up to M_s. At M_s the modes of the Lock and Sutherland models are transformed from subsonic to fast supersonic neutral modes.

Finally, figure 5 shows the variation of the phase speed of the neutral wave with Mach number for $\beta_T = 0.5$. This value of β_T is less than the transition value for the Tanh ($= 1.0$) and the Lock (≈ 0.57753) models but substantially greater than the transition value of the Sutherland model (≈ 0.164). Because of this, the results from the Tanh and Lock models are similar and both differ from those of the Sutherland model. Because the β_T of 0.5 is smaller than the transition values for the Tanh and Lock models the subsonic neutral modes of these models are transformed into slow

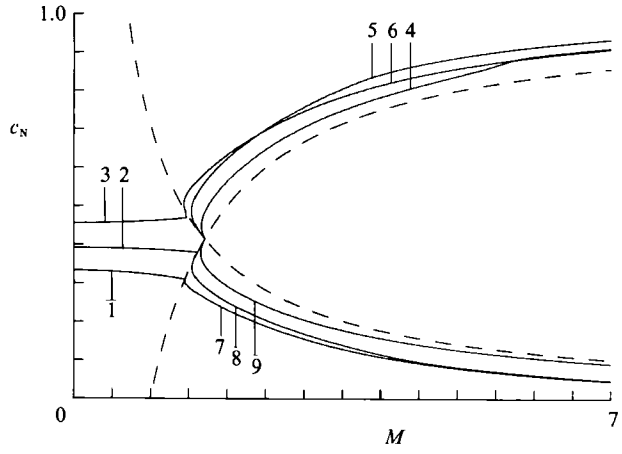

FIGURE 5. Plots of two-dimensional neutral phase speeds for $\beta_T = 0.5$ *vs.* Mach number: ——, phase and – – –, sonic speeds; subsonic modes: (1) Tanh, (2) Lock, (3) Sutherland; fast modes: (4) Tanh, (5) Lock, (6) Sutherland; slow modes: (7) Tanh, (8) Lock, (9) Sutherland.

supersonic neutral modes at M_s and fast supersonic neutral modes appear at M_*. Conversely, the subsonic neutral mode for the Sutherland model is transformed to a fast supersonic neutral mode at M_s, while a slow supersonic neutral mode appears at M_*. In regions 2 and 4 it can be seen that the phase speeds of the fast and slow supersonic neutral modes are quite similar for all models.

3.3. *Growth rates*

The maximum growth rates of the unstable modes are presented in this section and compared as a function of Mach number and β_T for the three models. In addition the variation of the growth rate with frequency for $\beta_T = 2.0$ is presented at selected values of the Mach number. It should be noted that the phase speeds of the unstable modes lie in the vicinity of the phase speed of the neutral mode in region 1 and between the phase speeds of the neutral modes and the corresponding sonic curves in regions 2 and 4. Thus we see that at any given Mach number there is only a small band of phase speeds of the unstable modes.

Figure 6 shows the maximum growth rates versus Mach number for $\beta_T = 2.0$. The general variation is similar for all of the models. The maximum growth rate is largest at Mach zero and decreases by a factor of 5 to 10 as the Mach number increases from zero to M_* and approaches a limiting value as the Mach number is further increased. At low Mach numbers the maximum growth rates for the Tanh model are the largest, followed in magnitude by those of the Sutherland and Lock models. At Mach numbers greater than M_* the Lock model has the largest growth rates of the fast supersonic modes while those of the Tanh and Sutherland models are roughly equal. The second group of unstable modes, the slow supersonic modes, appear at M_*. The growth rate of the most unstable of these modes first increases over a small range of Mach numbers and then levels off. At this value of β_T the maximum growth rates of these slow supersonic modes are about equal. In all cases, the maximum growth rate approaches a limiting value in this range of Mach numbers.

Similar results for $\beta_T = 1.0$ are shown in figure 7. In region 1 the growth rates obtained from the Tanh model are significantly larger than those of the other models. The maximum growth rates of these later two models are virtually identical in this

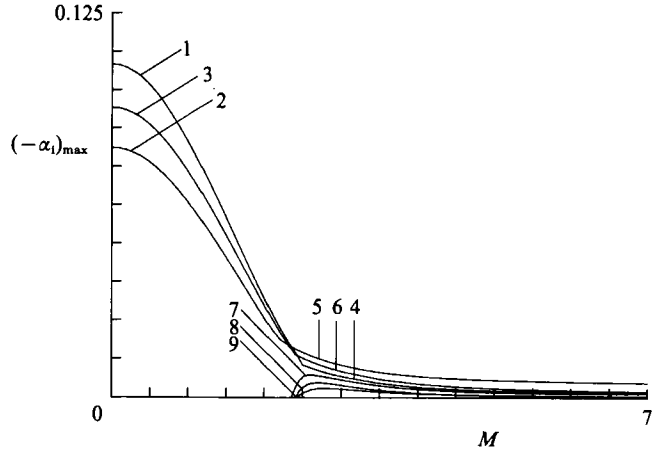

FIGURE 6. Plot of maximum growth rates of the two-dimensional modes *vs.* Mach number for $\beta_T = 2.0$; subsonic modes: (1) Tanh, (2) Lock, (3) Sutherland; fast modes: (4) Tanh, (5) Lock, (6) Sutherland; slow modes: (7) Tanh, (8) Lock, (9) Sutherland.

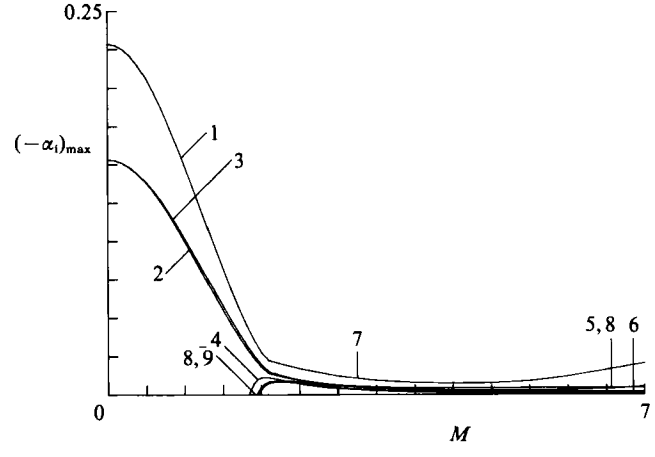

FIGURE 7. Plot of maximum growth rates of the two-dimension modes *vs.* Mach number for $\beta_T = 1.0$; subsonic modes: (1) Tanh, (2) Lock, (3) Sutherland; fast modes: (4) Tanh, (5) Lock, (6) Sutherland; slow modes: (7) Tanh, (8) Lock, (9) Sutherland.

region. Because this value of β_T corresponds to the transition value for the Tanh model, we see that the maximum growth rate of the subsonic mode and its slow supersonic continuation first decreases as the Mach number approaches M_*, levels off and then begins to increase with increasing Mach number. Because the transition values for the other two models are less than one, their behaviour is the same as in the previous case; the maximum growth rate decreases as the Mach number approaches M_* and then levels off for higher Mach numbers. Finally as in the previous case, the second group of unstable modes, those which appear at M_*, have maximum growth rates which are approximately equal and have similar behaviour.

The maximum growth rates for $\beta_T = 0.5$ are plotted versus the Mach number in figure 8. Note the change in scale of the maximum growth rate as β_T is decreased. It is important to realize that $\beta_T = 0.5$ is less than the transition value for both the

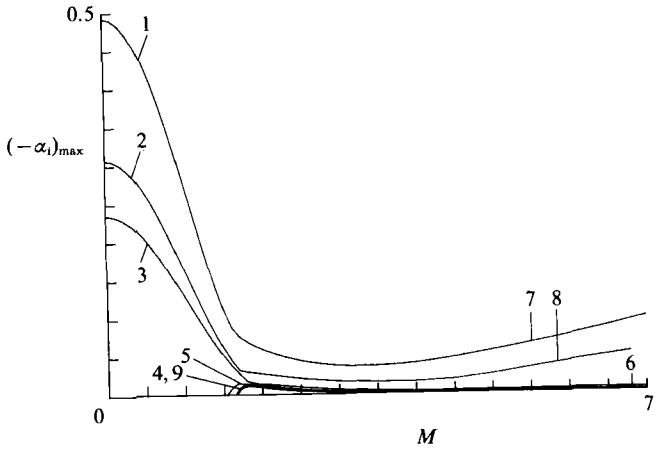

FIGURE 8. Plot of maximum growth rates of the two-dimensional modes *vs.* Mach number for $\beta_T = 0.5$; subsonic modes: (1) Tanh, (2) Lock, (3) Sutherland; fast modes: (4) Tanh, (5) Lock, (6) Sutherland; slow modes: (7) Tanh, (8) Lock, (9) Sutherland.

Tanh and Lock models but greater than that for the Sutherland model. Thus for the Tanh and Lock models the maximum growth rate decreases up to M_*, levels off and then increases with increasing Mach number. However, for the Sutherland model the behaviour is different because this value of β_T is larger than its transition value. Therefore, the variation with Mach number is the same as in the previous two cases. However, if the stationary gas were to be sufficiently cooled, we would expect that the maximum growth rate of the Sutherland model would behave in the same manner as the other two models at higher Mach numbers. Finally, as in the previous two cases, the second group of unstable modes have maximum growth rates which are approximately equal and have similar behaviour in this range of Mach numbers.

From the results given above, it is seen that the general variation of the maximum growth rate with Mach number depends on whether β_T is greater or less than its corresponding transition value. If $\beta_T > \hat{\beta}_T$, the growth rates of the unstable subsonic modes and their fast supersonic continuation first decrease as the Mach number is increased up to M_*, and then begin to level off. The growth rates of the slow supersonic modes which appear at M_*, first increase slightly, level off, and eventually increase with Mach number. If $\beta_T < \hat{\beta}_T$, the growth rates of the unstable subsonic modes and their slow supersonic continuation first decrease as the Mach number is increased up to M_*, level off, and then begin to increase with Mach number. The growth rates of the fast supersonic modes, which appear at M_*, first increase slightly then level off. We note that the maximum growth rates of the slow modes do not increase without bound as the Mach number is increased. Balsa & Goldstein (1990) have shown, for the Tanh model, that the growth rates decrease as $1/M$ for large enough Mach number. Thus the increase of the growth rates shown in the above figures will eventually level off and begin to decrease. In addition, the very high temperatures associated with large Mach numbers may invalidate these thermodynamic models because of the increasing importance of real gas effects.

Further insight into how the choice of thermodynamic model effects the growth rate of the unstable modes is provided by the results shown in figures 9 and 10. In these figures we show the variation of the growth rate of both the fast and slow unstable supersonic modes for $\beta_T = 2.0$ and $M = 2.5$ (figure 9) and $M = 5.0$ (figure 10)

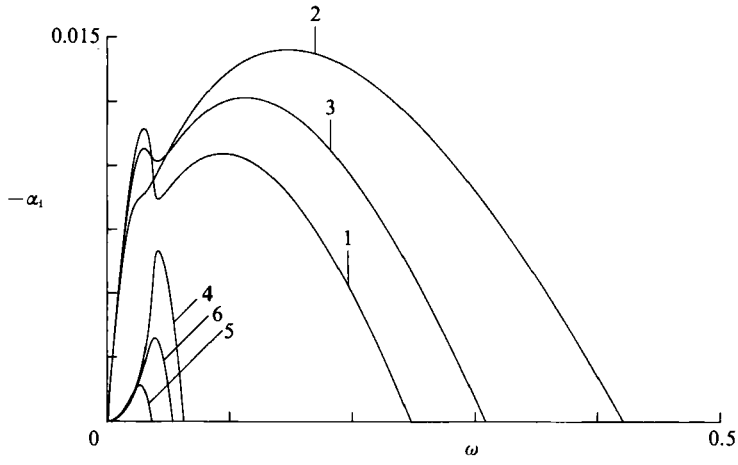

FIGURE 9. Plot of growth rates $-\alpha_i$ of the fast and slow two-dimensional modes *vs.* frequency for $\beta_T = 2$ and $M = 2.5$; fast modes: (1) Tanh, (2) Lock, (3) Sutherland; slow modes: (4) Tanh, (5) Lock, (6) Sutherland.

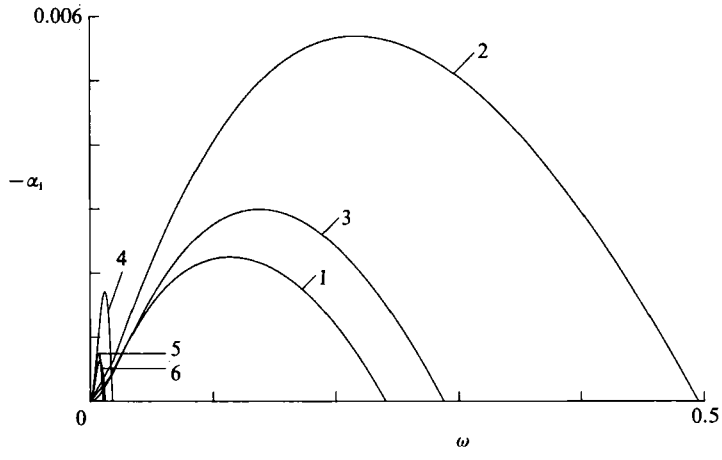

FIGURE 10. Plot of growth rates $-\alpha_i$ of the fast and slow two-dimensional modes *vs.* frequency for $\beta_T = 2$ and $M = 5.0$; fast modes: (1) Tanh, (2) Lock, (3) Sutherland; slow modes: (4) Tanh, (5) Lock, (6) Sutherland.

with the frequency of the disturbance. The results at Mach 2.5 show that the slow unstable supersonic modes exist in a very narrow range of frequencies compared to that of the unstable fast supersonic modes. The shape of the growth rate ($-\alpha_i$) versus frequency (ω) curves for the slow modes is similar for all of the models.

We found that the widest range of frequencies of the unstable slow supersonic modes and the maximum growth rates are those of the Tanh model, followed by those of the Sutherland model and then the Lock model. These results are somewhat different for the unstable fast supersonic modes, for which the Lock model has the largest maximum growth rates and the widest range of unstable frequencies. In terms of the maximum growth rates and range of unstable frequencies the Sutherland model is the next largest, followed by the Tanh model. Similar results for Mach 5 are shown in figure 10. Note the change in scales between these two figures.

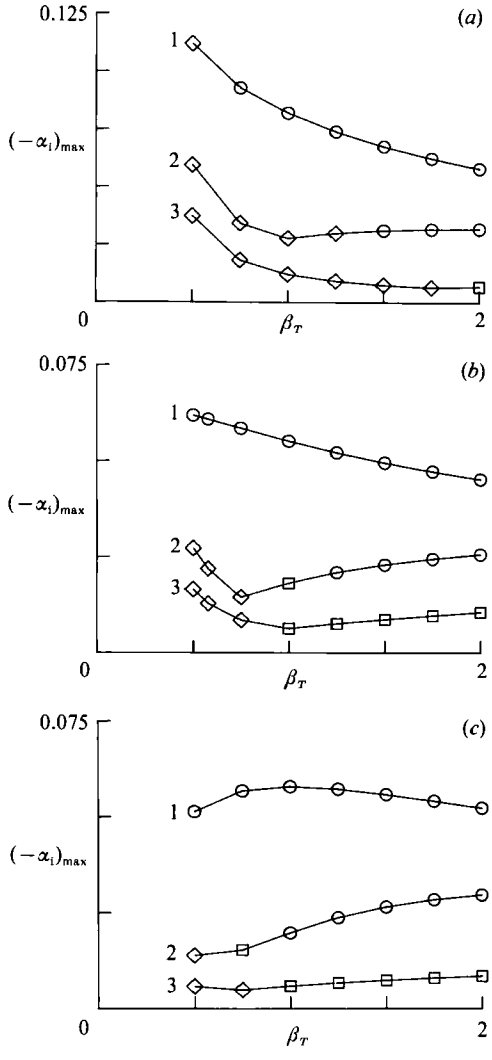

FIGURE 11. Plot of maximum growth rates versus β_T for Mach numbers (1) 1.5, (2) 2.0, (3) 3.0 for ○, subsonic; □, fast supersonic, and ◇, slow supersonic modes; (*a*) Tanh, (*b*) Lock, (*c*) Sutherland.

All of the features shown in the previous figure appear in this figure. The only exception is for the slow supersonic modes in which now the Lock model has a slightly larger growth rate than the Sutherland model. One striking feature of these results is the decrease in the range of frequencies of the slow mode.

The change in the overall maximum growth rate as a function of β_T at fixed Mach number is rather complex. This is due to the fact that for Mach numbers greater than M_* there are now two unstable modes, one in region 2 and another in region 4. An increase in β_T can result in a change in type of the most unstable mode. Some results bearing on this are shown in figure 11. Here we have plotted the maximum growth rate as a function of β_T for selected values of the Mach number for the three models. For example, at Mach 2 the most unstable mode for the Tanh model is a slow supersonic mode for values of β_T up to 1.25 while it is a subsonic mode for $\beta_T \geqslant 1.50$. For the Lock model, again at Mach 2, the most unstable mode is a slow supersonic

one up to $\beta_T = 0.75$, a fast supersonic mode at $\beta_T = 1.0$, and subsonic modes at values of β_T greater than or equal to 1.25. Finally, the Sutherland model at the same Mach number has, as its most unstable mode, a slow supersonic one at $\beta_T = 0.5$, a fast supersonic one at 0.75, and subsonic modes for β_T greater than or equal to 1.0. This change in mode type is related to the increase in M_* with increasing β_T independently of the thermodynamic model (see (2.12)). Thus as β_T is increased the extent of region 1 of the $c_r - M$ diagram increases so that unstable modes at fixed M can undergo a change from supersonic to subsonic.

4. Conclusions

The characteristic features of the solutions to the stability problem for the compressible mixing layer are qualitatively similar for all of the thermodynamic models used in this study. However, there are quantitative differences between the results obtained from the different models. These range from about 10% in the phase speeds to, in the most extreme case, about 50% difference in the maximum growth rates.

Despite these quantitative differences there is an underlying similarity in the qualitative behaviour of the solutions to the stability problem. For all three thermodynamic models the regularity condition yields a cubic in Mach number at fixed β_T. The behaviour of the solutions to the stability problem depends on whether β_T is larger or smaller than the transition value $\hat{\beta}_T$. If β_T is larger than $\hat{\beta}_T$ the subsonic modes are transformed into fast supersonic modes at the Mach number at which their phase speed equals that of the sonic wave in the stationary stream. On the other hand, if β_T is smaller than $\hat{\beta}_T$ the subsonic modes are transformed into slow supersonic modes when their phase speed equals the sonic speed of the moving stream. If $\beta_T = \hat{\beta}_T$, then the phase speeds of the subsonic neutral modes are constant. This mode splits into a pair of fast and slow supersonic modes at M_*. For any value of β_T there is a single band of unstable subsonic modes in region 1, but there are two bands of unstable supersonic modes, one in region 2 and one in region 4. For all of the thermodynamic models, the second band of unstable supersonic modes appears when the Mach number equals M_*. These second modes are slow supersonic modes if $\beta_T > \hat{\beta}_T$ and fast supersonic modes if $\beta_T < \hat{\beta}_T$. Both the fast and slow unstable supersonic modes have a rather small variation in the phase speed about the mean value. Finally, we note that the value of $\hat{\beta}_T$ is a sensitive function of the Prandtl number for the Sutherland model.

We have found that, independent of the thermodynamic model, the maximum growth rates of the unstable modes decrease by a factor of 5 to 10 as the Mach number is increased from zero to M_*. As the Mach number is increased beyond M_* the maximum growth rates of the fast supersonic modes approach a limiting value. On the other hand, the maximum growth rates of the slow supersonic modes first level off for $M > M_*$ and then begin to increase with a further increase in the Mach number.

In view of the results presented here we conclude that all of the thermodynamic models yield qualitatively similar results. In view of this, all previous work based on simplified thermodynamic models yields qualitatively correct results. Because of the analytical simplicity of the Tanh model and because it appears to be a reasonable approximation to the mean velocity and temperature profiles we suggest that it is appropriate for use in non-parallel and nonlinear models of the stability of the compressible mixing layer.

This work was supported by the National Aeronautics and Space Administration under NASA Contract NAS1-18605 while the authors were in residence at the Institute for Computer Applications in Science and Engineering, NASA Langley Research Center, Hampton, VA 23665, USA.

REFERENCES

Balsa, T. F. & Goldstein, M. E. 1990 On the instabilities of supersonic mixing layers: A high-Mach-number asymptotic theory. *J. Fluid Mech.* **216**, 585–611.

Blumen, W. 1970 Shear layer instability of an inviscid compressible fluid. *J. Fluid Mech* **40**, 769–781.

Blumen, W., Drazin, P. G. & Billings, D. F. 1975 Shear layer instability of an inviscid compressible fluid. Part 2. *J. Fluid Mech.* **71**, 305–316.

Brown, W. B. 1962 Exact numerical solutions of the complete linearized equations for the stability of compressible boundary layers. *Norair Rep.* NOR-62-15, Northrop Aircraft Inc., Hawthorne, CA.

Chapman, D. R. 1950 Laminar mixing of a compressible fluid. *NACA Rep.* 958.

Djordjevic, V. D. & Redekopp, L. G. 1988 Linear stability analysis of nonhomentropic, inviscid compressible flows. *Phys. Fluids* **31**, 3239–3245.

Drazin, P. G. & Davey, A. 1977 Shear layer instability of an inviscid compressible fluid. Part 3. *J. Fluid Mech.* **82**, 255–260.

Drazin, P. G. & Reid, W. H. 1984 *Hydrodynamic Stability.* Cambridge University Press.

Gill, A. E. 1965 Instabilities of 'top-hat' jets and wakes in compressible fluids. *Phys. Fluids* **8**, 1428–1430.

Gropengiesser, H. 1969 On the stability of free shear layers in compressible flows. (In German), Deutsche Luft. und Raumfahrt, FB 69-25, 123 pp. Also, *NASA Tech. Trans.* F-12,786.

Jackson, T. L. & Grosch, C. E. 1989 Inviscal spatial stability of a compressible mixing layer. *J. Fluid Mech.* **208**, 609–637.

Jackson, T. L. & Grosch, C. E. 1990*a* On the classification of unstable modes in bounded compressible mixing layers. In *Instability and Transition* (ed. M. Y. Hussaini & R. G. Voigt), pp. 187–198. Springer.

Jackson, T. L. & Grosch, C. E. 1990*b* Inviscid spatial stability of a compressible mixing layer. Part 2. The flame sheet model. *J. Fluid Mech.* **217**, 391–420.

Klemp, J. B. & Acrivos, A. 1972 A note on the laminar mixing of two uniform parallel semi-infinite streams. *J. Fluid Mech.* **55**, 25–30.

Lees, L. & Lin, C. C. 1946 Investigation of the stability of the laminar boundary layer in a compressible fluid. *NACA Tech. Note* 1115.

Lees, L. & Reshotko, E. 1962 Stability of the compressible laminar boundary layer. *J. Fluid Mech.* **12**, 555–590.

Lessen, M., Fox, J. A. & Zien, H. M. 1965 On the inviscid stability of the laminar mixing of two parallel streams of a compressible fluid. *J. Fluid Mech.* **23**, 355–367.

Lessen, M., Fox, J. A. & Zien, H. M. 1966 Stability of the laminar mixing of two parallel streams with respect to supersonic disturbances. *J. Fluid Mech.* **25**, 737–742.

Lock, R. C. 1951 The velocity distribution in the laminar boundary layer between parallel streams. *Q. J. Mech. Appl. Maths* **4**, 42–63.

Macaraeg, M. G., Streett, C. L. & Hussaini, M. Y. 1988 A spectral collocation solution to the compressible stability eigenvalue problem. NASA Tech. Paper 2858.

Mack, L. M. 1965 Computation of the stability of the laminar compressible boundary layer. In *Methods in Computational Physics* (ed. B. Alder, S. Fernbach & M. Rotenberg), vol. 4, pp. 247–299. Academic.

Mack, L. M. 1984 Boundary layer linear stability theory. In *Special Course on Stability and Transition of Laminar Flow. AGARD Rep.* R-709, 3.1–3.81.

Mack, L. M. 1987 Review of linear compressible stability theory. In *Stability of Time Dependent and Spatially Varying Flows* (ed. D. L. Dwoyer & M. Y. Hussaini), pp. 164–187. Springer.

MACK, L. M. 1989 On the inviscid acoustic-mode instability of supersonic shear flows. *Fourth Symp. Numer. Phys. Aspects of Aerodyn. Flows.* California State University, Long Beach, California.

RAGAB, S. A. & WU, J. L. 1988 Instabilities in the free shear layer formed by two supersonic streams. *AIAA Paper* 88-0038.

STEWARTSON, K. 1964 *The Theory of Laminar Boundary Layers in Compressible Fluids.* Oxford University Press.

TAM, C. K. W. & HU, F. Q. 1988 Instabilities of supersonic mixing layers inside a rectangular channel. *AIAA Paper* 88-3675.

TAM, C. K. W. & HU, F. Q. 1989 The instability and acoustic wave modes of supersonic mixing layers inside a rectangular channel. *J. Fluid Mech.* **203**, 51–76.

TING, L. 1959 On the mixing of two parallel streams. *J. Math. Phys.* **28**, 153–165.

ZHUANG, M., KUBOTA, T. & DIMOTAKIS, P. E. 1988 On the instability of inviscid, compressible free shear layers. *AIAA Paper* 88-3538.